Sensors and Actuators B 203 (2014) 655–662

Contents lists available at ScienceDirect

Sensors and Actuators B: Chemical

journal homepage: www.elsevier.com/locate/snb

Simultaneous electroanalytical determination of luteolin and rutin using artificial neural networks

Alvaro Yamil Tesio[a,1], Sebastián Noel Robledo[b], Adrian Marcelo Granero[a], Héctor Fernández[a,*], María Alicia Zon[a,*]

[a] Departamento de Química, Facultad de Ciencias Exactas, Físico-Químicas y Naturales, Universidad Nacional de Río Cuarto, 5800 Río Cuarto, Córdoba, Argentina
[b] Departamento de Tecnología Química, Facultad de Ingeniería, Universidad Nacional de Río Cuarto, 5800 Río Cuarto, Córdoba, Argentina

ARTICLE INFO

Article history:
Received 5 March 2014
Received in revised form 24 June 2014
Accepted 2 July 2014
Available online 10 July 2014

Keywords:
Flavonoids
Luteolin
Rutin
SWV
Modified electrodes
ANNs

ABSTRACT

In this study, we propose an electroanalytical method to quantify simultaneously luteolin and rutin, two flavonoids which are present in a pharmaceutical formulation. The methodology is based on square wave voltammetry at glassy carbon electrodes modified with multiwalled carbon nanotubes dispersed in polyethylenimine. Both flavonoids show quasi-reversible surface redox couples in 10% ethanol + 1 mol L^{-1} $HClO_4$ aqueous solutions, which are defined in potential regions very close to each other. The adsorption process of flavonoids on the modified electrode surface was carried out using an accumulation potential of 0.55 V (vs. Ag/AgCl, 3 mol L^{-1} KCl), and an accumulation time of 20 min.

Considering that luteolin and rutin electrochemical responses show a high degree of overlapping, we processed the electrochemical signals using artificial neural networks. We used a supervised network, feed-forward network with Levenberg-Marquardt back propagation training. Values of 92.6 ± 0.4 and 92 ± 1 mg per tablet were determined by the artificial neural networks methodology for luteolin and rutin, respectively. According to values declared by the manufacturer, differences of 7.4 and 8.0% were calculated for luteolin and rutin, respectively. Results obtained with electroanalytical methodologies were in very good agreement with those obtained by HPLC.

1. Introduction

Flavonoids are benzo-γ-pyrone derivatives containing piranic and phenolic rings in their molecular structures. In most of the cases, flavonoids are molecules that have two benzene rings (A and B) linked through a chain of three carbon atoms (ring C when carbon atoms form a cycle). Flavonoids are extensively found in nature such as in fruits, seeds, and vegetables [1].

Luteolin (3′,4′,5,7-tetrahydroxy-flavone; LUT) belongs to the subclass of flavonoids known as flavones and is rated as one of the most bioactive flavonoids. It is found mainly in parsley, celery, thyme, and peanut hulls [2]. Its chemical structure is shown in Fig. 1a. LUT has a resorcinol group in the benzene ring A, and a catechol group in the benzene ring B. LUT has beneficial effects on human health, such as cardiovascular protection, anti allergic, and anticancer activities, anti-ulcer effects, and prevent cataracts [3]. LUT also inhibits platelet aggregation by vasodilating action [4].

Rutin (3′,4′,5,7-tetrahydroxyflavone-3-O-β-D-rutinoside; RU) (Fig. 1b), a natural flavone derivative, is also considered one of the most bioactive flavonoids [5]. RU has different physiological activities such as anti-inflammatory, anti-tumor, anti-bacterial, antioxidant, and anti-allergic. RU also acts as a stimulant of the immune system [6], and has several pharmacological activities, including vaso-active, anti-viral and anti-protozoal [7].

Flavonoids have mainly been determined in fruits, vegetables and different beverages by reverse-phase high-performance liquid chromatography (HPLC) with ultraviolet detection [8], coulometric array detection [9] or amperometric detection [10], and to a lesser extent, using various other techniques, such as: spectrophotometry, thin-layer chromatography (TLC), gas chromatography (GC), capillary electrophoresis (CE) and electrochemical methods [11].

The LUT analytical determination has been reported by TLC [12], GC [13], gas chromatography–mass spectrometry (GC-MS) [14],

* Corresponding authors. Tel.: +54 358 4676 440; fax: +54 358 4676 233.
E-mail addresses: alvaro_tesio@hotmail.com (A.Y. Tesio), srobledo@ing.unrc.edu.ar (S.N. Robledo), agranero@exa.unrc.edu.ar (A.M. Granero), hfernandez@exa.unrc.edu.ar (H. Fernández), azon@exa.unrc.edu.ar, alicia_zon@hotmail.com (M.A. Zon).
[1] Present address: INQUIMAE (CONICET), Facultad de Ciencias Exactas y Naturales, Universidad de Buenos Aires, Pabellón 2, Ciudad Universitaria, Buenos Aires, Argentina.

http://dx.doi.org/10.1016/j.snb.2014.07.005
0925-4005/

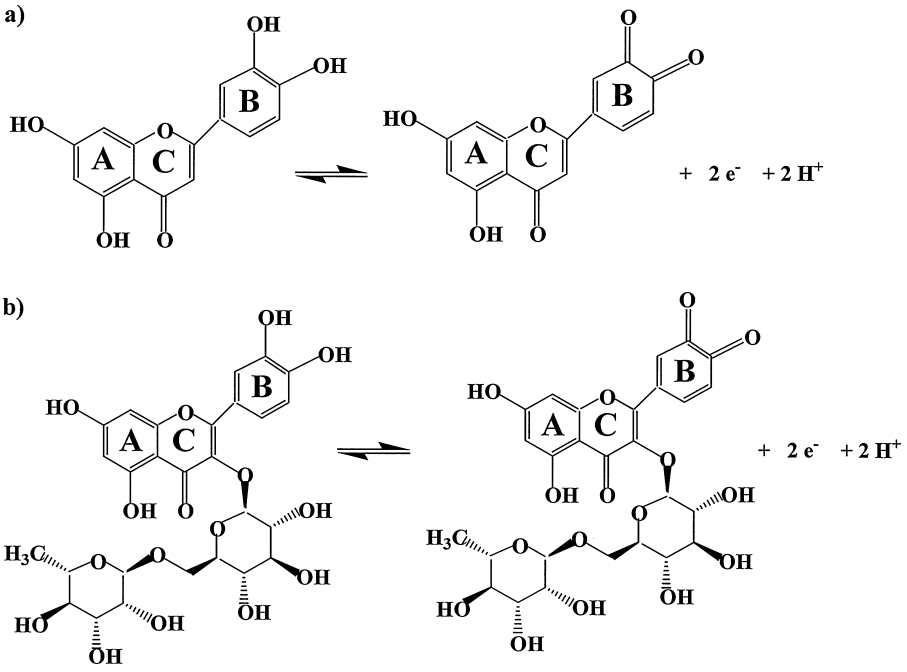

Fig. 1. Chemical structures of flavonoids and products of the first peak of electrochemical oxidation of luteolin (a) and rutin (b).

HPLC [15–18], and CE [19] coupled with various detection techniques, such as UV spectrometry, electrochemical, etc.

The RU analytical determination has been carried out using different methodologies such as spectrometry [20,21], HPLC [22], CE [23], and chemiluminescence [24].

The electrochemical behavior of RU has been studied at electrodes of different materials such as bare glassy carbon [25], hanging mercury drop [26], and gold electrodes modified with single-walled carbon nanotubes [27]. In addition, electrochemical sensors and biosensors for the RU determination have been described in the literature [28,29].

On the other hand, several chemometric tools have been described to resolve systems where signals appear overlapped [30]. The most used chemometric techniques are deconvolution [31], multivariate curve resolution [32,33], and multivariate calibration [34,35]. The most popular chemometric tools are, particularly, in the field of electrochemistry, multivariate calibration based on different regression methods such as multilinear regression (MLR) [36], principal component regression (PCR) [37], continuum regression [38], partial least squares regression (PLS-1) [39], and artificial neural networks (ANNs) [30,40].

In addition, ANNs is a data processing system consisting of a large number of highly interconnected elements in an architecture inspired by the structure of the brain, and it is a powerful modeling tool for processing from complex to imprecise data [41]. The ANNs processing systems can be performed using a conventional set of independent analyses. However, it could be advantageous to replace this with a statistically designed experimental procedure in which several factors are simultaneously varied. This multivariate approach reduces the number of experiments and improves statistical interpretation of results [42].

In this study, we propose the simultaneous determination of LUT and RU in a pharmaceutical formulation at glassy carbon electrodes (GCE) modified with multi-walled carbon nanotubes (MWCNTs) dispersed in polyethylenimine (PEI) in 10% ethanol + 1 mol L^{-1} $HClO_4$ aqueous solution using cyclic (CV), and square wave (SWV) voltammetries. Electrochemical impedance spectroscopy (EIS) is also used to compare the state of bare and modified GCE. Considering that surface voltammetric signals of LUT and RU show a high overlapping, we used the ANNs methodology, and an experimental design to quantify the LUT and RU content in the pharmaceutical formulation. For comparison purposes, these studies were also carried out using HPLC.

2. Materials and methods

2.1. Reagents

LUT, RU, and a dispersion of PEI in water were purchased from Sigma–Aldrich. MWCNTs (diameter 30 ± 15 nm, length 1–5 μm) were obtained from Nano-Lab (USA). $HClO_4$, ethanol, methanol, and acetic acid were Merck p.a. Acetonitrile was Sintorgan, HPLC degree. Ultrapure water (ρ = 18 MΩ cm) was obtained from a Millipore-Milli Q system. Stock solutions of LUT (3.5×10^{-3} mol L^{-1}) and RU (8.7×10^{-4} mol L^{-1}) were prepared in ethanol, protected from light, and kept in the refrigerator. They were stable for at least two months. Working solutions were prepared daily by adding different aliquots of stock solutions to 1 mol L^{-1} $HClO_4$ aqueous solutions. The percentage of ethanol in all solutions was 10%.

2.2. Apparatus

CV and SWV experiments were performed with an Epsilon (BAS, USA) Potentiostat. EIS measurements were carried out in solutions containing equal concentrations (1×10^{-3} mol L^{-1}) of oxidized and reduced forms of the $[Fe(CN)_6]^{4-/3-}$ redox couple, with 0.1 mol L^{-1} KCl as the supporting electrolyte. EIS experiments were performed with an AutoLab PGSTAT 30 potentiostat, controlled by FRA 4.9 software. A 5 mV amplitude sine wave perturbation was applied to the electrode, whereas the dc potential was set at the formal potential of the redox couple, i.e., $E_f^o = 0.240$ V vs. Ag/AgCl. The ac frequency was varied from 0.5 Hz to 10 kHz. Both, the in-phase (Z') and out of phase (Z'') impedance components were extracted from the experimental data. Values of the electron-transfer resistance (R_{ct}), and double layer capacitance (C_{dl}) for both the bare and modified GCE were extracted from a non-linear squares fitting

to the classical Randles' circuit [43], which is incorporated into the FRA electrochemical impedance software. Electrochemical measurements were carried out in a 5 mL Pyrex cell. Working electrodes were GCE (CH Instruments, area = 0.071 cm^2) modified with MWCNTs dispersed in PEI (GCE/MWCNTs-PEI). A platinum wire and an Ag/AgCl, 3 mol L^{-1} NaCl (BAS, RE-5B) were used as counter and reference electrodes, respectively.

HPLC measurements were carried out using a Waters 2998 system equipped with a quaternary pump model Waters e2695, diode array detector, and a C18 (Luna) column (100 mm × 4.6 mm). The injection volume was 15 μL. The mobile phase flow rate was kept constant at 0.5 mL min^{-1}. An elution gradient was used, starting with 60% of solvent A (H_2O/acetic acid (99:1)) and 40% solvent B (methanol/acetonitrile/acetic acid (89:10:1)), and was varied linearly up to 100% solvent B in 30 min.

2.3. Preparation of GCE/MWCNTs-PEI electrodes

The GCE was pre-treated by polishing with alumina slurries of 1, 0.3 and 0.05 μm for 1 min each, and sonicated in a water bath during 15 s.

MWCNTs-PEI dispersions were obtained by mixing 1.0 mg of MWCNTs with 1.0 mL of PEI solutions of different concentrations prepared in 50:50 (v/v) ethanol/water, followed by sonication during 45 min. The MWCNTs–PEI ratio which allowed obtaining the best electrochemical signal was 1:5; i.e., 1.0 mg of MWCNTs with 5 mg PEI per mL [44]. The polished GCE was modified with the MWCNTs-PEI dispersion by dropping an aliquot of 20 μL on the top of the electrode and allowing drying during 90 min at room temperature.

We have previously studied the electrochemical behavior of LUT surface redox couple at both the modified GCE and the bare GCE [44]. A much better definition of this surface redox couple was found at the modified GCE in comparison with the bare GCE, with an increase of about 20% in current intensities. A similar behavior was found for RU surface redox couple. Based on these results, we perform present studies at GCE/MWCNTs/PEI electrodes.

2.4. Sample preparation

One tablet of LutiMax (SYNORx Inc., San Clemente, California, USA) was finely milled and transferred to a volumetric flask, and dissolved in 25 mL of ethanol. This solution was immersed in an ultrasonic bath during 120 s, and then was filtered. Then, different aliquots of the solution were added to 1 mol L^{-1} $HClO_4$ aqueous solution, and transferred to the electrochemical cell. The simultaneous determination of LUT and RU was performed using adsorptive stripping SWV using ANNs.

LUT and RU contents were 100 mg each per LutiMax tablet, according to the manufacturer.

2.5. Experimental procedure

The CGE/MWCNTs–PEI electrode was cycled 10 times from −0.2 to 0.9 V in 1 mol L^{-1} $HClO_4$ aqueous solution at a scan rate, υ = 0.050 V s^{-1}. Then, the GCE/MWCNTs–PEI electrode was immersed in 10% ethanol + 1 mol L^{-1} $HClO_4$ aqueous solutions containing LUT or RUT or LUT + RU (at given concentrations). Optimal conditions for LUT and RU accumulation on the modified electrode surface were an accumulation potential of 0.55 V, and an accumulation time of 20 min under stirring at 800 rpm. Finally, the voltammetric stripping was performed in the same solution. Voltammograms were recorded in the potential range from 0 to 0.8 V. Other experimental parameters were the amplitude of the square wave, ΔE_{sw} = 0.025 V, the staircase potential, ΔE_s = 0.005 V and the frequency, f = 100 Hz. In CV, the scan rate (υ) was varied from 0.025 to 0.200 V s^{-1}.

Table 1
Concentration values of LUT and RU in 10% ethanol + 1 mol L^{-1} $HClO_4$ aqueous solution used as output data in the calibration set (samples 1–10) and the validation set (samples 11–19).

Samples	$c^*_{LUT} \times 10^6$(mol L^{-1})	$c^*_{RU} \times 10^6$(mol L^{-1})
1	60	120
2	60	3.4
3	120	60
4	60	60
5	100	100
6	100	20
7	3.4	60
8	20	20
9	20	100
10	60	60
11	75	75
12	5.0	5.0
13	5.0	75
14	40	5.0
15	75	40
16	40	40
17	40	75
18	5.0	40
19	75	5.0

Complex impedance plots are shown in Fig. S1 (Supplementary Material) for both bare GCE and GCE/MWCNTs/PEI electrode. A semicircle portion is defined at higher frequencies in both electrodes, which corresponds to the electron-transfer limited process, followed by a linear part at lower frequencies attributable to diffusion [43]. Values of 175 ± 2 Ω and 0.98 ± 0.02 μF were obtained for R_{ct} and C_{dl}, respectively, from the best fitting of experimental data for the bare GCE. On the other hand, values of 30 ± 1 Ω and 1.9 ± 0.1 μF were determined for R_{ct} and C_{dl}, respectively, for the GCE/MWCNTs/PEI electrode. These results clearly show that the presence of MWCNTs at the modified electrode to decrease the resistance to charge transfer and increases the double layer capacitance, which are in good agreement with results previously obtained by us [44], and other discussed in literature [45].

Supplementary Fig. S1 related to this article can be found, in the online version, at http://dx.doi.org/10.1016/j.snb.2014.07.005.

Pure nitrogen was bubbled in the solutions for at least 10 min prior to measurements. The temperature was 25 °C.

2.6. Chemometric calculations

2.6.1. Preparation of standards

Standard solutions were prepared by mixing aliquots of different concentrations of LUT (c^*_{LUT}) and RU (c^*_{RU}) in 10% ethanol + 1 mol L^{-1} $HClO_4$ aqueous solution (Table 1). Samples 1–10 were designed to obtain the calibration set. Their concentrations were established through an experimental design for two factors, "central composite" of type "2^2 + star", rotatable, and with two central points (Fig. 2a) in the concentration range from 2.0×10^{-5} to 1.0×10^{-4} mol L^{-1} for both substrates.

Samples 11–19 were designed to obtain the validation set. Concentration values were chosen using of a factorial design of 3-levels with two factors (3^2) (Fig. 2b) in a concentration range from 5.0×10^{-6} to 7.5×10^{-5} mol L^{-1} for both substrates.

2.6.2. Software's

The Neural Network toolbox from the software suite MATLAB 7.8 [46] was used for applications of ANNs.

An algorithm also written in MATLAB was used for generating ellipses [47].

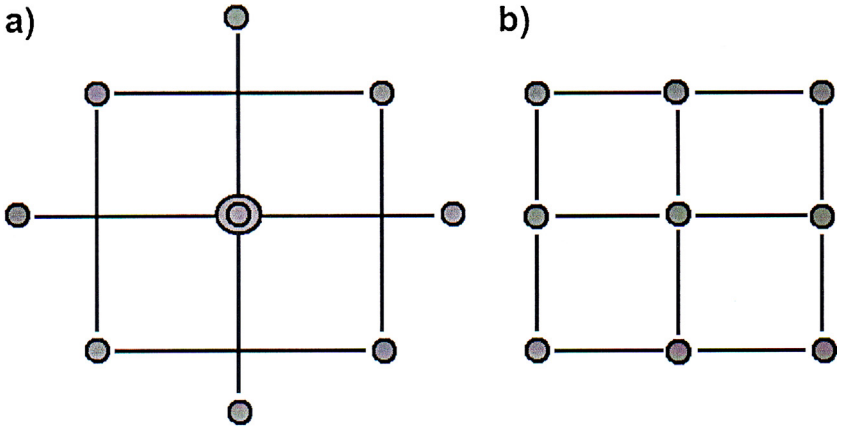

Fig. 2. Response surface designs. (a) Design "central composite" of type "2^2 + star", rotatable, and with two central points, and (b) factorial design of 3-levels with 2 factors (3^2).

2.6.3. Applications of ANNs

The problem presented in this study is one case of generalization, trying to predict concentrations of LUT and RU based on SW voltammograms.

We compared different architectures to build and validate the predictive model of the network, which consisted of an input layer, one hidden and one output. The number of neurons of the input layer was equal to the number of independent variables entered into the model, in this case 101 parameters obtained from voltammetric responses, and the number of neurons in the output layer corresponded to the number of model output variables, i.e., concentrations of LUT and RU (Table 1).

On the other hand, the number of neurons in the hidden layer was that obtained from the best architecture of ANNs through the following procedure: (1) we created an ANNs with a number N of neurons in the hidden layer. (2) It was defined the type of training and the transfer function. (3) The network was trained with the calibration data set, considering a 70% of learning, a 15% for monitoring, and another 15% to test the network. (4) The network was validated using the validation data set (independent set of calibration data), and (5) root mean square error (RMSE) values were obtained from points three and four.

The above procedure was made by combining different types of training and transfer functions. After obtaining the errors of different architectures, we selected the best amount of the hidden layer neurons, the transfer function, and the training type based on the least mean squared normalized error (MSE), the percentage relative errors (RE%), relative errors of predictions (REP%), and rmse for two substrates, avoiding the overfitting (see below).

2.6.4. Validation of results

To evaluate the quality of quantitative predictions of concentrations obtained from the ANNs, the RMSE between nominal and estimated concentrations for each substrate, RE% and REP% were calculated by applying Eqs. (1)–(3), respectively:

$$\mathrm{RMSE} = \sqrt{\frac{\sum_{i=1}^{n}(\hat{c}_i - c_i)^2}{n}} \quad (1)$$

$$\mathrm{RE}(\%) = 100\sqrt{\frac{\sum_{i=1}^{n}(\hat{c}_i - c_i)^2}{\sum_{i=1}^{n}c_i^2}} \quad (2)$$

$$\mathrm{REP}(\%) = \frac{100}{c_{\mathrm{mean}}}\sqrt{\frac{\sum_{i=1}^{n}(\hat{c}_i - c_i)^2}{n}} \quad (3)$$

where $\hat{c}_i$ and c_i are estimated and nominal concentrations, respectively, and c_{mean} is the mean of nominal concentrations.

In addition, a procedure to verify if the point (1,0) is contained in the confidence elliptical region of the slope and the intercept of the fitted curve between nominal and estimated concentrations was used to evaluate whether or not these concentrations differ statistically [30,48].

3. Results and discussion

3.1. Quantification of luteolin and rutin in a pharmaceutical formulation using SWV and ANNs

The pharmaceutical formulation contains mainly two flavonoids, i.e., LUT and RU.

A cyclic voltammogram, and net currents (I_n) of a SW voltammogram recorded at GCE/MWCNTs-PEI electrodes for the ethanol extract obtained from the pharmaceutical formulation are shown in Fig. 3a and b, respectively. In both cases, only one oxidation peak was found. Plots of anodic peak currents as a function of v obtained from cyclic voltammograms of the ethanol extract were linear (linear correlation coefficient, $r = 0.9998$) as it is theoretically expected for an adsorption controlled redox process [43]. It is also known that the first oxidation peak of all flavonoids with a Catechol group in B ring shows a behavior that can be described as a reversible or quasi-reversible process, involving $2e^-$, $2H^+$ [49]. Chemical structures of products of the first peak of LUT and RU electrochemical oxidation are shown in Fig. 1a and b, respectively.

On the other hand, cyclic and square wave voltammograms recorded in an equimolar mixture of LUT and RU showed also one single peak (results not shown). The overlapping of voltammetric signals can be explained considering that RU structure differs of LUT by only one extra glucoside in the ring C (Fig. 1).

Current vs. concentration relationships of mixtures of both flavonoids were first analyzed by PLS-1 through MVC1 [50]. From merit figures, and error indicator based on deviations of net signal linearity, and sensor selection could be inferred a behavior away from linearity.

Based on these results, we applied the ANNs methodology to determine of LUT and RU in the pharmaceutical formulation. Therefore, SW voltammograms of LUT and RU solutions described in Table 1 were recorded at GCE/MWCNTs-PEI electrodes. Fig. 4a shows SW voltammograms obtained for samples 1–10 of Table 1 after subtracting the blank currents, which were used to obtain the calibration model. In addition, Fig. 4b shows SW voltammograms obtained for samples 11–19 of Table 1, which were used in the validation model (see below).

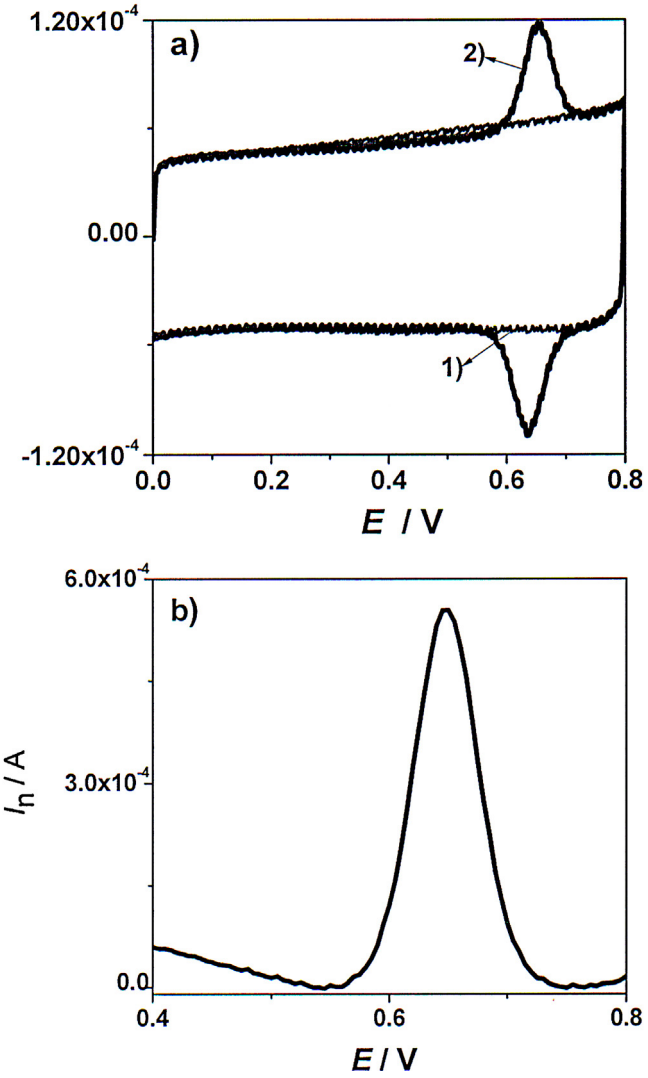

Fig. 3. (a) Cyclic voltammograms of the blank solution (1) and the LutiMax ethanol extract (2) at the GCE/MWCNTs–PEI electrode in 1 mol L^{-1} $HClO_4$. $\upsilon = 0.050\ V\ s^{-1}$. (b) SW voltammogram recorded for the same extract under the same experimental conditions. $\Delta E_{sw} = 0.025$ V, $\Delta E_s = 0.005$ V, $f = 100$ Hz.

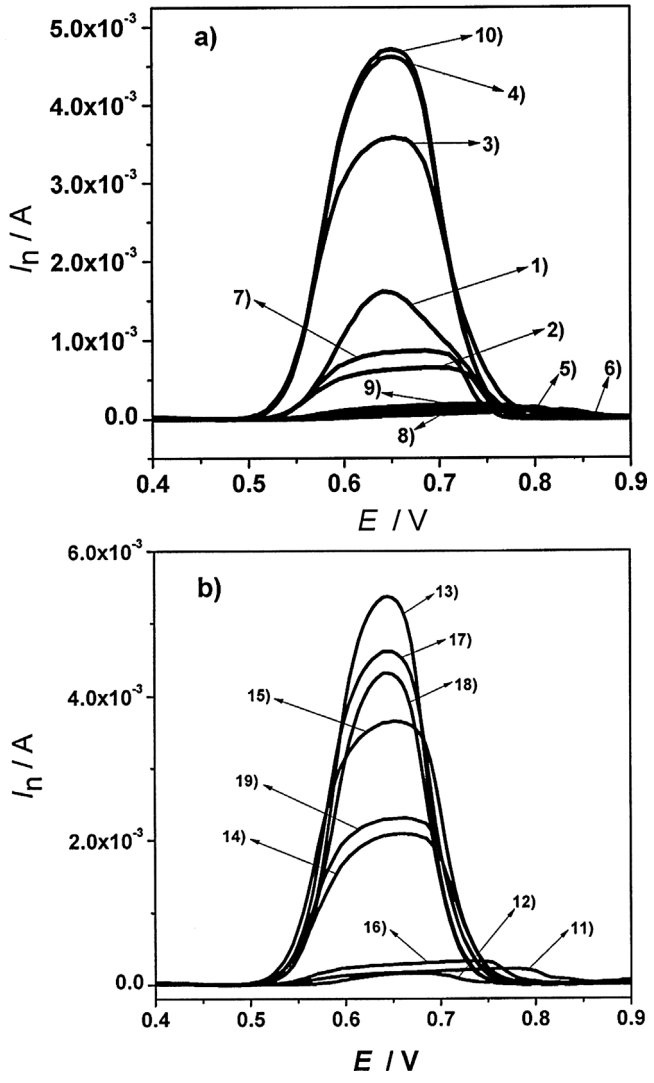

Fig. 4. Square wave voltammograms of solutions used in (a) the calibration set (samples 1–10 in Table 1) and (b) the validation set (samples 11–19 in Table 1).

Therefore, we applied the methodology previously explained to find the most suitable network architecture for the resolution of measured signals. Thus, the best network model was obtained using a 101-7-2 architecture, i.e., 101 neurons in the input layer, 7 in the hidden layer, and 2 in the output layer. We used Tansig sigmoid transfer function in the hidden layer, and the Purelin linear function for the output layer. The most appropriate algorithm in the training stage was that of Levenberg-Marquardt [46].

As previously described, the number of neurons of the input layer was equal to the number of independent variables entered into the model. In this case, 101 parameters obtained from voltammetric responses, and the number of neurons in the output layer corresponded to the number of model output variables, i.e., nominal concentrations of LUT and RU.

Optimized parameters, and errors estimated from ANNs methodology are shown in Tables 2 and 3, respectively.

Plots of the estimated concentrations vs. nominal concentrations are shown in Fig. 5a and b for LUT and RU, respectively. Table 4 shows the linear regression parameters and associated errors.

After optimizing the ANNs with the set of calibration, we used a separate set of voltammograms to perform the validation step through the analysis of accuracy and precision. The linear

Table 2
Optimized parameters of ANNs.

Architecture	101-7-2
Number of iterations	80
Hidden layer transfer function	Tansing
RMSETr, C[a]	1.80×10^{-11}
RSMEM, C[b]	2.38×10^{-10}
RSMET, C[c]	1.86×10^{-10}

[a] RMSE for training for the calibration set.
[b] RMSE for monitoring for the calibration set.
[c] RMSE for test for the calibration set.

Table 3
Errors estimated for the simultaneous determination of LUT and RU by ANNs.

	LUT	RU
RMSE, C[a]	2.45×10^{-6}	7.26×10^{-6}
RMSE, P[b]	2.04×10^{-6}	3.38×10^{-6}
REP (%)	5.1	8.4
Average recovery	101 (2)[c]	101.2 (0.2)[c]

[a] RMSE for calibration set.
[b] RMSE for prediction set.
[c] Values in parentheses are standard deviations.

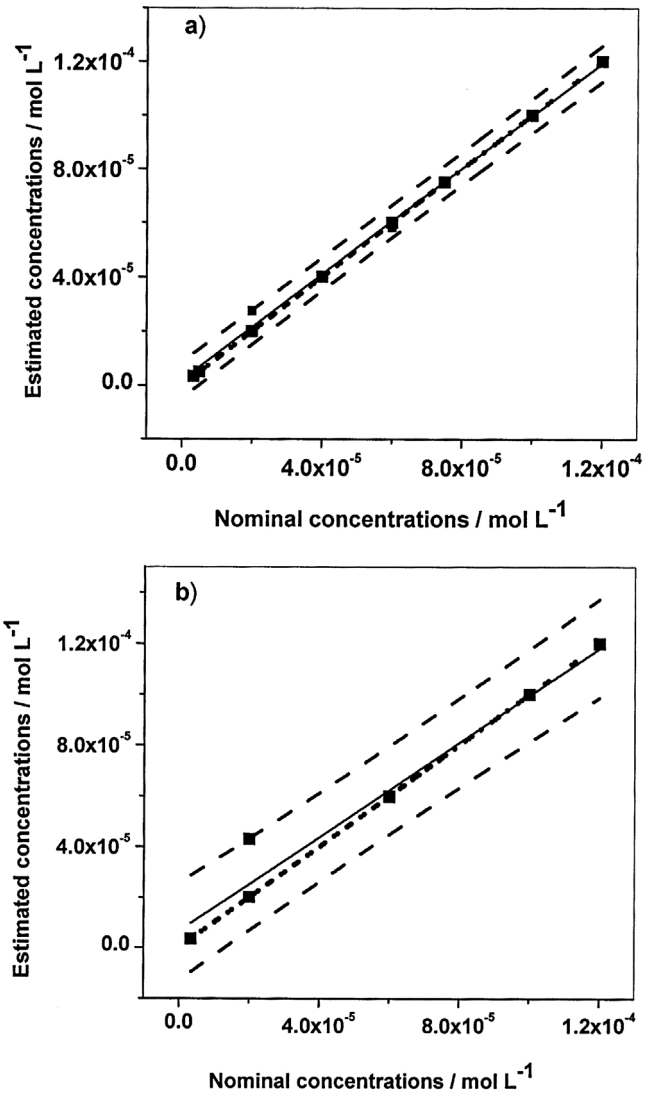

Fig. 5. Comparison between estimated values obtained by ANNs and nominal concentrations using the calibration set for (a) LUT and (b) RU. Solid and dotted lines represent the fitted and ideal regressions, respectively, with the corresponding prediction bands at a confidence level of 95% (dashed lines).

Table 4
Linear regression parameters obtained from the dependence between nominal concentrations and estimated concentrations by ANNs.

Flavonoid	Intercept (mol L^{-1})	Slope	r^a	RE (%)
LUT	$(2.0 \pm 1.5) \times 10^{-6}$	0.98 ± 0.02	0.9980	1.28
RU	$(6.5 \pm 4.4) \times 10^{-6}$	0.93 ± 0.06	0.9825	3.80

[a] r is the linear correlation coefficient.

regression parameters, and associated errors obtained from plots of estimated concentrations as a function of nominal concentrations of the validation set (samples 11–19 in Table 1) were: slope = 1.10 ± 0.29, intercept = (0.01 ± 0.01) × 10^{-5} mol L^{-1}, and the linear correlation coefficient, r = 0.9509 for LUT. For RU these values were slope = 0.99 ± 0.34, intercept = (−0.3 ± 0.1) × 10^{-5} mol L^{-1}, and r = 0.9347. However, as the slope and the intercept are not statistically independent variables since there is always some degree of correlation between them. Thus, it is better to analyze if the point (1,0) was included in the elliptical region of the joint confidence of slope and intercept in order to evaluate whether or not concentrations estimated by the ANNs method differ statistically from nominal concentrations. Plots of ellipses obtained from the validation set are shown in Fig. 6 for each substrate. Results obtained for LUT and RU by the ANNs method include the ideal point, exhibiting a comparable accuracy for both substrates, and a greater precision for LUT. Thus, the ANNs method is adequate as a calibration model to determine LUT and RU in the real sample.

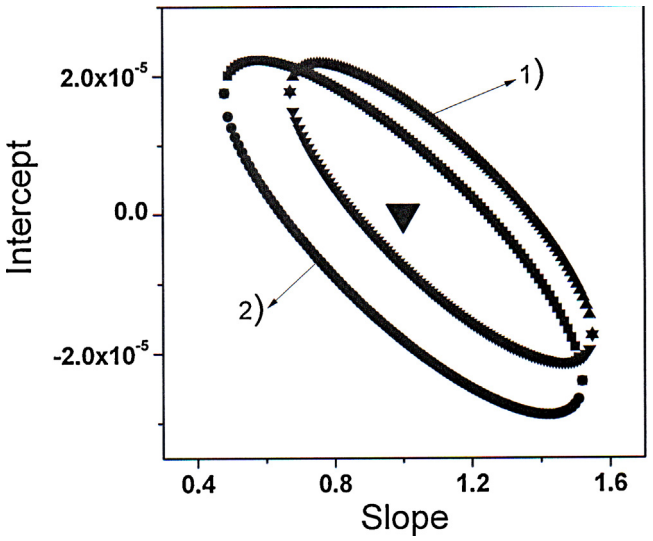

Fig. 6. Elliptical regions of the joint confidence obtained by ANNs from the validation set for (1) LUT and (2) RU. (▼) is the ideal point (1,0).

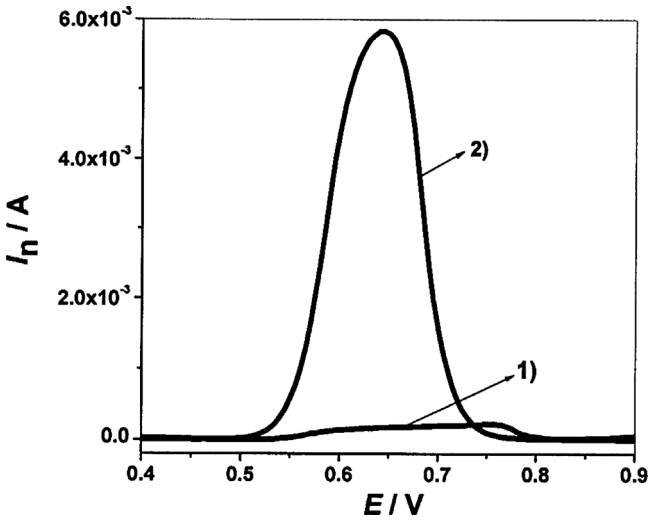

Fig. 7. Square wave voltammograms recorded for two ethanol LutiMax extracts at different concentrations of the extract. (1) LutiMax 1 and (2) LutiMax 2 (see Table 4).

Table 5
Results obtained in the determination of LUT and RU in the pharmaceutical formulation.

	Nominal concentrations		Estimated concentrations	
	LutiMax 1	LutiMax 2	LutiMax 1	LutiMax 2
c^*_{LUT} (mol L^{-1})	9.00×10^{-5}	4.00×10^{-5}	8.36×10^{-5}	3.81×10^{-5}
c^*_{RU} (mol L^{-1})	4.20×10^{-5}	1.87×10^{-5}	3.83×10^{-5}	1.74×10^{-5}

Finally, we calculated concentrations of LUT and RU in two different LutiMax ethanol extracts (LutiMax 1 and LutiMax 2). SW voltammograms used are shown in Fig. 7. Results obtained are summarized in Table 5. We used two ethanol extracts to demonstrate that the results obtained were independent of the concentration levels of the substrates.

Calculated values for LUT and RU concentrations in the pharmaceutical formulation were 92.6 ± 0.4 and 92 ± 1 mg per tablet, respectively. These results are close to the content of LUT and RU declared by the manufacturer, with a difference of −7.4 and −8% for LUT and RU, respectively.

3.2. Quantification of luteolin and rutin in the pharmaceutical formulation using HPLC

For comparison purposes, the LUT and RU content in the pharmaceutical formulation was also determined by HPLC. Retention times were 28.5 and 18.9 min for LUT and RU, respectively.

Calibration curves were constructed using peak area values of LUT and RU. For LUT, peak areas were analyzed at $\lambda = 349$ nm, the wavelength at which LUT presents a maximum absorption in ethanol. The calibration curve was expressed as: intercept $= -(2 \pm 1) \times 10^5$ AU min^{-1}, slope $= (6.3 \pm 0.3) \times 10^{10}$ AU min^{-1} mol^{-1} L, $r = 0.9948$ and the experimental statistical parameter $F = 1.513$, where AU are absorbance units. For RU, areas of chromatographic peaks were analyzed at $\lambda = 356$ nm, since this is the wavelength of maximum absorption of RU in ethanol. The calibration curve gave the following values: intercept $= -(4 \pm 3) \times 10^5$ AU min^{-1}, slope $= (8.3 \pm 0.2) \times 10^{10}$ AU min^{-1} mol^{-1} L, $r = 0.9981$ and $F = 0.991$. F values show that both calibration curves comply with the linearity test. Using the corresponding calibration curves, values obtained for LUT and RU were 93 ± 8 and 96 ± 4 mg ($n = 3$) by tablet, respectively, in very good agreement with those values obtained using SWV and ANNs. Thus, the percentage relative errors for the determination of LUT and RU between chromatographic and electrochemical methods were 0.4 and 4%, respectively.

Thus, the methodology proposed here is simple and fast, the relative cost compared to chromatography is considerably smaller, it could be applicable for portable designs, and presents very good analytical parameters. The method was useful for the quantification of LUT and RU in a pharmaceutical formulation with excellent agreement with the values determined by HPLC. Based on these results, we can conclude that adsorptive stripping SWV coupled to ANNs could provide a satisfactory methodology for LUT and RU determination in pharmaceutical formulation samples and potentially for other real samples.

4. Conclusions

Adsorptive Stripping Square Wave Voltammetry coupled to the Artificial Neural Networks methodology were successfully used to determine the luteolin and rutin content in a pharmaceutical formulation, following a very simple extraction procedure. In addition, results obtained with these methodologies were in excellent agreement with those obtained using the chromatographic method. This good analytical performance allowed us to determine the content of luteolin and rutin in a pharmaceutical formulation, providing an advantageous alternative to existing methods for the determination of luteolin and rutin in real samples.

Acknowledgements

Financial support from Agencia Nacional de Promoción Científica y Tecnológica FONCYT (PICT 0916/10), Consejo Nacional de Investigaciones Científicas y Técnicas CONICET (PIP 112-200801-01993), Ministerio de Ciencia y Tecnología de la Provincia de Córdoba (MINCyT), and Secretaría de Ciencia y Técnica (SECyT) from Universidad Nacional de Río Cuarto is gratefully acknowledged. A. Y. Tesio and S. N. Robledo thank to CONICET for postdoctoral fellowships.

References

[1] G. Di Carlo, N. Mascolo, A.A. Izzo, F. Capasso, Flavonoids: old and new aspects of a class of natural therapeutic drugs, Life Sci. 65 (1999) 337–353.
[2] J. Pokorny, N. Yanishlieva, M. Gordon, Antioxidantes de los alimentos. Aplicaciones prácticas, Acribia S. A., Zaragoza, España, 2001.
[3] M. López-Lázaro, Distribution and biological activities of the flavonoid luteolin, Mini Rev. Med. Chem. 9 (2009) 31–59.
[4] V.R. Sánchez de Rojas, B. Somoza, T. Ortega, A.M. Villar, Different mechanisms involved in the vasorelaxant effect of flavonoids isolated from satureja obovata, Planta Med. 62 (1996) 554–556.
[5] R. Mauludin, R.H. Müller, C.M. Keck, Development of an oral rutin nanocrystal formulation, Int. J. Pharm. 370 (2009) 202–209.
[6] M.L. Calabró, S. Tommasini, P. Donato, R. Stancanelli, D. Raneri, S. Catania, C. Costa, V. Vilari, P. Ficarra, R. Ficarra, The rutin/beta-cyclodextrin interactions in fully aqueous solution: spectroscopic studies and biological assays, J. Pharm. Biomed. Anal. 36 (2005) 1019–1027.
[7] W. Panasiak, M. Wleklik, A. Oraczewska, M. Luczak, Influence of flavonoids on combined experimental infections with EMC virus and Staphylococcus aureus in mice, Acta Microbiol. Pol. 37 (1989) 185–188.
[8] V. Kuntić, N. Pejić, B. Ivković, Z. Vujić, K. Ilić, S. Mićić, V. Vukojević, Isocratic RP-HPLC method for rutin determination in solid oral dosage forms, Pharm. Biomed. Anal. 43 (2007) 718–722.
[9] P. Gamache, E. Ryan, I. Acworth, Analysis of phenolic and flavonoid compounds in juice beverages using HPLC with coulometric array detection, J. Chromatogr. 635 (1993) 143–150.
[10] L. Wu, J.B. Laughlin Jr., H.D. Dewald, Voltammetry and LCEC of isoflavones, Electroanalysis 9 (1997) 796–799.
[11] C.D. Stalikas, Extraction, separation, and detection methods for phenolic acids and flavonoids, J. Sep. Sci. 30 (2007) 3268–3295.
[12] I. Fecka, W. Cisowski, TLC determination of tannins and flavonoids in extracts from some Erodium species using chemically modified stationary phases, J. Planar Chromatogr. 15 (2002) 429–432.
[13] C.S. Liu, Y.S. Song, K.J. Zhang, J.C. Ryu, M. Kim, T.U. Zhou, Gas chromatographic/mass spectrometric profiling of luteolin and its metabolites in rat urine and bile, J. Pharm. Biomed. Anal. 13 (1995) 1409–1414.
[14] Z. Füzfai, I. Molnár-Perl, Gas chromatographic–mass spectrometric fragmentation study of flavonoids as their trimethylsilyl derivatives: analysis of flavonoids, sugars, carboxylic and amino acids in model systems and in citrus fruits, J. Chromatogr. A 1149 (2007) 88–101.
[15] H. Srinivasa, M.S. Bagul, H. Padh, M. Rajani, A rapid densitometric method for the quantification of luteolin in medicinal plants using HPTLC, Chromatographia 60 (2004) 131–134.
[16] D.R. Jin, H. Hakamata, K. Takahashi, A. Kotani, F. Kusu, Separation of flavonoids by semi-micro high-performance liquid chromatography with electrochemical detection, Bull. Chem. Soc. Jpn. 77 (2004) 1147–1152.
[17] Z.M. Qian, H.J. Li, P. Li, M.T. Ren, D. Tang, Simultaneous qualitation and quantification of thirteen bioactive compounds in Flos Lonicerae by high-performance liquid chromatography with diode array detector and mass spectrometry, Chem. Pharm. Bull. 55 (2007) 1073–1076.
[18] Y.Z. Zhou, X.X. Liu, X.H. Zheng, J.B. Zheng, Simultaneous determination of quercetin and luteolin in dried flowers by multivariate HPLC-ECD calibration, Chromatographia 66 (2007) 635–637.
[19] Q.C. Chu, L.M. Jiang, J.N. Ye, Determination of phenols in Fructus Lycii by capillary electrophoresis with electrochemical detection, J. Anal. Chem. 65 (2010) 103–108.
[20] K. Lavanya, T.R. Baggi, Spectrophotometric determination of rutin in pharmaceutical preparations using 3-methylbenzthiazolinone-2-hydrazone, Microchem. J. 41 (1990) 126–131.
[21] H.N.A. Hassan, B.N. Barsoum, I.H.I. Habib, Simultaneous spectrophotometric determination of rutin, quercetin and ascorbic acid in drugs using a Kalman filter approach, J. Pharm. Biomed. Anal. 20 (1999) 315–320.
[22] K. Ishii, T. Furuta, Y. Kasuya, Determination of rutin in human plasma by high-performance liquid chromatography utilizing solid-phase extraction and ultraviolet detection, J. Chromatogr. B 759 (2001) 161–168.
[23] M. Polášek, I. Petriška, M. Pospíšilová, L. Jahodář, Use of molybdate as novel complex-forming selector in the analysis of polyhydric phenols by capillary zone electrophoresis, Talanta 69 (2006) 192–198.
[24] Z. Song, S. Hou, Sensitive determination of sub-nanogram amounts of rutin by its inhibition on chemiluminescence with immobilized reagents, Talanta 57 (2002) 59–67.
[25] F.E. Aragao Catunda Jr., M.F. de Araujo, A.M. Granero, F.J. Arévalo, M.G. de Carvalho, M.A. Zon, H. Fernández, The redox thermodynamics and kinetics of flavonoid rutin adsorbed at glassy carbon electrodes by stripping square wave voltammetry, Electrochim. Acta 56 (2011) 9707–9713.
[26] A.A. Ensafi, R. Hajian, Determination of rutin in pharmaceutical compounds and tea using cathodic adsorptive stripping voltammetry, Electroanalysis 18 (2006) 579–585.
[27] B. Zeng, S. Wei, F. Xiao, F. Zhao, Voltammetric behavior and determination of rutin at a single-walled carbon nanotubes modified gold electrode, Sens. Actuators B: Chem. 115 (2006) 240–246.
[28] J-L. He, Y. Yang, X. Yang, Y-L. Liu, Z-H. Liu, G-L. Shen, R-Q. Yu, β-Cyclodextrin incorporated carbon nanotube-modified electrode as an electrochemical sensor for rutin, Sens. Actuators B: Chem. 114 (2006) 94–100.

[29] C. Mousty, S. Cosnier, M.S-P. López, E. López-Cabarcos, B. López-Ruiz, Rutin determination at an amperometric biosensor, Electroanalysis 19 (2007) 253–258.
[30] A.C. Olivieri, H.C. Goicoechea, La calibración en Química Analítica, Ediciones UNL, Universidad Nacional del Litoral, Santa Fe, Argentina, 2007.
[31] H.L. Surprenant, T.H. Ridgway, C.N. Reilley, Convolution and deconvolution in the synthesis and analysis of staircase voltammograms, J. Electroanal. Chem. 75 (1977) 125–134.
[32] M.B. Mamián-López, R.J. Poppi, Standard addition method applied to the urinary quantification of nicotine in the presence of cotinine and anabasine using surface enhanced Raman spectroscopy and multivariate curve resolution, Anal. Chim. Acta 760 (2013) 53–59.
[33] C. Ruckebusch, L. Blanchet, Multivariate curve resolution: a review of advanced and tailored applications and challenges, Anal. Chim. Acta 765 (2013) 28–36.
[34] G.M. Escandar, P.C. Damiani, H.C. Goicoechea, A.C. Olivieri, A review of multivariate calibration methods applied to biomedical analysis, Microchem. J. 82 (2006) 29–42.
[35] C. Zapata-Urzúa, M. Pérez-Ortiz, M. Bravo, A.C. Olivieri, A. Álvarez-Lueje, Simultaneous voltammetric determination of levodopa, carbidopa and benserazide in pharmaceuticals using multivariate calibration, Talanta 82 (2010) 962–968.
[36] C. Bessant, S. Saini, A chemometric analysis of dual pulse staircase voltammograms obtained in mixtures of ethanol, fructose and glucose, J. Electroanal. Chem. 489 (2000) 76–83.
[37] Y.S. Zhong, Y.N. Ni, S. Kokot, Application of differential pulse stripping voltammetry and chemometrics for the determination of three antibiotic drugs in food samples, Chin. Chem. Lett. 23 (2012) 339–342.
[38] M.C. Ortiz, J. Arcos, L. Sarabia, Using continuum regression for quantitative analysis with overlapping signals obtained by differential pulse polarography, Chemom. Intell. Lab. Syst. 34 (1996) 245–262.
[39] Y. Ni, Y. Wang, S. Kokot, Simultaneous determination of three fluoroquinolones by linear sweep stripping voltammetry with the aid of chemometrics, Talanta 69 (2006) 216–225.
[40] S.N. Robledo, V.G.L. Zachetti, M.A. Zon, H. Fernández, Quantitative determination of tocopherols in edible vegetable oils using electrochemical ultra-microsensors combined with chemometric tools, Talanta 116 (2013) 964–971.
[41] G. Hanrahan, Computational neural networks complex analytical problem solving, Anal. Chem. 82 (2010) 4307–4313.
[42] C.R.T. Tarley, G. Silveira, W.N.L. dos Santos, G.D. Matos, E.G.P. da Silva, M.A. Bezerra, M. Miró, S.L. Costa Ferreira, Chemometric tools in electroanalytical chemistry: methods for optimization based on factorial design and response surface methodology, Microchem. J. 92 (2009) 58–67.
[43] A.J. Bard, L.R. Faulkner, Electrochemical Methods: Fundamentals and Applications, 2nd ed., Marcel Dekker, New York, 2001.
[44] A.Y. Tesio, A.M. Granero, N.R. Vettorazzi, N.F. Ferreyra, G.A. Rivas, H. Fernández, M.A. Zon, Development of an electrochemical sensor for the determination of the flavonoid luteolin in peanut hull samples, Microchem. J. 115 (2014) 100–105.
[45] F. Gutierrez, M.D. Rubianes, G.A. Rivas, Dispersion of multi-wall carbon nanotubes in glucose oxidase: characterization and analytical applications for glucose biosensing, Sens. Actuators B: Chem. 161 (2012) 191–197.
[46] Mathworks, Description of the Neural Network Toolbox. Toolbox NN v6.0.3. Design and Simulate Neural Networks, 2010, http://www.mathworks.com/products/neural-network/
[47] http://www.fbcb.unl.edu.ar/catedras/analitica
[48] J. Riu, F.X. Rius, Assessing the accuracy of analytical methods using linear regression with errors in both axes, Anal. Chem. 68 (1996) 1851–1857.
[49] S.M. Golabi, L. Irannejad, Preparation and electrochemical study of fisetin modified glassy carbon electrode. Application to the determination of NADH and ascorbic acid, Electroanalysis 17 (2005) 985–996.
[50] A.C. Olivieri, H.C. Goicoechea, F.A. Iñón, MVC1, an integrated MatLab toolbox for first-order multivariate calibration, Chemmom. Intell. Lab. Syst. 73 (2004) 189–197.

Biographies

Alvaro Y. Tesio obtained his degree in Chemistry (2008) from Río Cuarto National University (Río Cuarto, Argentina) and his Ph.D. in Chemistry (2013) in the group of Electroanalysis at the Chemistry Department, Faculty of Exact, Physicochemical and Natural Sciences (Río Cuarto National University). Now he has a postdoctoral fellowship from Argentine Research Council (CONICET) working at Buenos Aires University-INQUIMAE. His research is focus on Oxygen Reduction Reaction (ORR), basic understanding of lithium-air batteries chemistry and its application for new technologies.

Sebastián N. Robledo obtained his Ph.D. in Chemistry (2012) from Rio Cuarto National University (UNRC) (Río Cuarto, Argentina). Now, he is carrying out a postdoctoral work in the Group of Electroanalysis at the Chemistry Department, Faculty of Exact, Physicochemical, and Natural Sciences (UNRC). Currently, he has a postdoctoral fellowship from Argentine Research Council (CONICET) at the same Department. He is Assistant Professor at Faculty of Engineering (UNRC). His research interest focus on several subjects, such as electrochemistry of mycotoxins and synthetic and natural antioxidants, studies on ultramicroelectrodes and their use for electroanalytical applications, and artificial neuronal networks.

Adrian M. Granero obtained his Ph.D. in Chemistry (2009) from Río Cuarto National University (UNRC, Río Cuarto, Argentina). He is actually doing a Postdoctoral training (2009–2012) at Río Cuarto National University, and at Córdoba National University (UNC, Córdoba, Argentina). Currently, is Assistant Researcher at Argentine Research Council (CONICET). His research interest focus on several subjects, such as electrochemistry of mycotoxins, natural antioxidants, and the design of sensors/biosensors for the determination of these substances in real matrixes. Actually, he has over eleven peer-reviewed papers and two book chapters.

Héctor Fernández obtained his Ph.D. in Chemistry (1978) from Rio Cuarto National University (UNRC, Río Cuarto, Argentina). He carried out a Postdoctoral training (1980–1982) at University of New York at Buffalo, USA. Now, he is a Full Professor at UNRC and Principal Researcher at Argentine Research Council (CONICET). His research interest focus on electrochemistry of mycotoxins, hormones and natural antioxidants studies on nano-structured electrodes, and the development of electroanalytical techniques for the determination of these substances in real matrixes. Design and characterization of chemical sensors, electrochemical (bio)sensors and immunoelectrodes based on nano-structured materials. He has over seventy peer-reviewed papers and three book chapters and has been the editor of an electroanalytical book.

María A. Zon obtained her Ph.D. in Chemistry (1985) from Rio Cuarto National University (Río Cuarto, Argentina). She carried out a postdoctoral training at Cordoba University (Córdoba, Spain) between 1990 and 1992. She is Full Professor at Rio Cuarto National University and Principal Researcher at Argentine Research Council (CONICET). Her researches focus in the development of electrochemical (bio) sensors by using nano-materials for the determination of different substrates, such as mycotoxins, antioxidants and hormones. She has over sixty peer-reviewed papers and three book chapters. She has been co-editor of an electroanalytical book.